Simplified Design and Optimization of Slotless Synchronous PM Machine for Micro-Satellite Electro-Mechanical Batteries

Babak ABDI[1], Jafar MILIMONFARED[1], Javad SHOKROLLAHI MOGHANI[1], Ali KASHEFI KAVIANI[2]
[1]*Elec. Eng. Dep. Amirkabir University of Technology, Tehran, Iran.*
[2] *Elec. Eng. Dep. Florida International University, Miami, Florida, USA.*
babakabdi@ieee.org

***Abstract*—Electro-mechanical batteries have important advantages as compared with chemical batteries, especially in low earth orbit satellites applications. High speed slotless external rotor permanent magnet machines are used in these systems as Motor/Generator. Proper material and structure for space applications are introduced. A simplified analytic design method is given for this type of machines. Finally, the optimization of machine in order to have maximum efficiency and minimum volume and weight are given in this paper. Particle swarm optimization is used as the optimization algorithm and the finite element-based simulations are used to confirm the design and optimization process and show less than 1.2% error in parametric design.**

***Index Terms*—Flywheel, Electromechanical, battery, energy storage, slotless, design**

I. INTRODUCTION

Flywheel energy storage systems or Electro-Mechanical Batteries (EMBs) were introduced by Maryland University [1] and NASA [2] in 1970s. Recently, they are most commonly used in Low Earth Orbit (LEO) satellites. Nano/micro satellites are usually included in LEO satellites, which rotate around the earth from some minutes to a few hours. Despite the development of chemical batteries technology, the most critical part of these satellites is their energy storage system. Their life is limited by fast charge/discharge rating in such applications [3].

Rotational kinetic energy is stored in a high-speed flywheel in EMBs. The advantages of EMBs are presented in [1]-[6]. Unlimited charge/discharge cycle as well as the satellite lifetime, higher efficiency, higher energy density, higher discharge depths, thermal independency and their usage in attitude control of satellite can be mentioned among these advantages. Instruction for design and optimization of flywheel to achieve lower stress and weight for space applications are presented in [4], [5].

Figure 1 shows a block diagram of a LEO satellite electrical subsystem using EMB. Solar cells supply loads and also charge EMB during the day. EMB supply the loads during eclipse and discharge as well, periodically. A bidirectional DC-DC converter is used for solar cell Maximum Power Tracking (MPT) and boosting the amplitude of DC bus voltage to proper value for EMB in charge duration. It is a buck converter in discharge duration and decrease EMB voltage to the DC bus value. The electrical machine used in EMB is a 3 phase variable speed machine. So, a proper drive subsystem is used for inverting DC voltage to variable frequency, 3 phase voltage in the charge duration and vice versa in discharge period. Finally EMB is used as energy storage system. It contains an electrical machine surrounded by flywheel, magnetic bearings and case [2]. Figure 2 shows the electrical machine integrated with the flywheel. The most important part of an EMB is the electrical machine, which is used as Motor/Generator for energy conversion. Synchronous Permanent Magnet (SPM) machines are mostly used in EMBs because of the high torque to weight ratio, low rotor losses, high efficiency and brushless ness. Consequently, they are introduced and proposed to be used in EMBs in [5].

From another point of view, slotless PM machines have some advantages over slotted PM machines. Lower stator losses and no cogging torque can be mentioned as their most important privileges. So, slotless PM machines are suggested for high-speed applications [7]-[11]. According to Figure 2, the effective air gap in slotless machines includes air gap in addition to copper thickness. The large air-gap causes magnetic flux weakening in this kind of machines. Therefore, in high power machines they would not be the best choice because of non-optimal mass and volume. However, in low power applications in which efficiency is important, like micro-satellite EMBs, the slotless machines are preferred to the slotted ones.

In [12]-[14] some analytical models were presented but they were too complex for the design and optimization process. In this paper, a simple design method will be presented by assuming proper approximation for air-gap magnetic flux density. This approximation causes less than 6% error in the design process but it highly simplifies the design process.

Results of design and optimization process are validated using Finite Element Method (FEM) simulations to ensure low errors. Two-dimensional static and AC simulations are used to achieve this aim. Ansoft Maxwell-2D software is used for FEM simulations.

Particle Swarm Optimization (PSO) will be used for the machines optimization because of its advantages like fast convergence and continuity [15].

Proper material and machine structure for space applications will be presented in section II. Simplified design is given in section III, optimization process results with PSO algorithm are given in sections IV. FEM simulations confirm the design and optimization process in section V and section VI presents conclusions of the paper.

Digital Object Identifier 10.4316/AECE.2009.03015

II. SELECTION OF MATERIAL AND CONSTRUCTION

A. Material selection

Motor/Generator used in micro-satellite EMB is a variable high-speed small electrical machine with some limitations such as thermal, and heat transfer, volume and mass. Rotor or flywheel is floated by magnetic bearings and rotor dissipations are excreted by radiation. Therefore, the PMs installed on rotor surface are subjected to high temperature with wide variations range. Then, the suitable PM for this application is samarium-cobalt (Sm-Co) which has high energy density and good performance stability against the temperature variations [5]. Ferromagnetic material used in stator and rotor back irons is chosen based on their losses at working point and saturation level. Among ferromagnetic materials, Iron-cobalt and amorphous iron are the candidates. Amorphous iron is chosen because of its lower losses. Kapton is appropriate for electrical insulation and Litz wires are used for skin effect reduction [5, 16].

B. Proper structure

Stored kinetic energy in a flywheel is related to inertia and square of angular velocity ($0.5I\omega^2$). On the other hand, inertia is related to the mass and square of flywheel radius (mr^2). Then, the angular velocity and radius have to be kept as large as possible for the optimum volume and mass. So, proper structure for micro-satellite EMBs is a hollow cylinder with centered external rotor electrical machine as shown in Figure 1.

The method of PM installation on rotor is another important parameter. Surface mounted permanent magnet machines are suitable because of higher energy density and lower harmonic production [17]. The final important parameter to select a proper structure is the pole numbers. Two or four pole machines are used for high speed applications to minimize the core losses, but the torque produced by a four pole machine is more than two times with respect to the two pole machine [5], [18], and [19]. Consequently, proper pole number for micro-satellite EMB is chosen to be four.

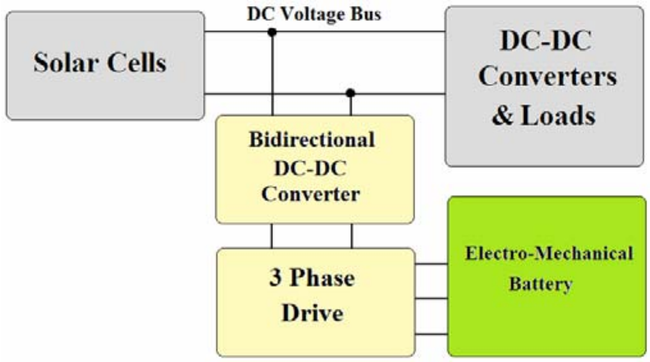

Figure 1. Electrical power subsystem of a LEO satellite using EMB.

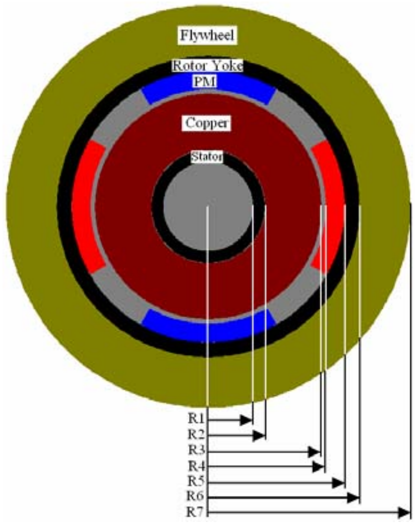

Figure 2. Electro-mechanical Battery under design.

TABLE I
UNDER DESIGN EMB PARAMETERS

Output Power (Watt)	Charge/discharge time (sec.)	Min speed (rpm)	Max speed (rpm)	Min line voltage (v)	Max line voltage (v)
40	1800	20000	60000	24	72
Pole number	Filling-factor	air gap (mm)	Bmaxr (T)	R1 (mm)	
4	0.5	1	1.5	10	

III. SIMPLIFIED DESIGN

Analytical design of external rotor permanent magnet machine are given here. It will be done on the basis of Figure 2 for the specifications given in Table I. The simple analytical design proposed here is suitable for optimization. It is simplified using acceptable approximations.

Design process of permanent magnet machines for EMB application can be organized as follows:

- Determination of flux density functions in the air gap.
- Calculation of current and winding turn-number according to the required torque and output voltage.
- Calculation of necessary Iron area to have the working point below the saturation or optimum flux density point.
- Calculation of necessary copper area based on to the copper and insulators area and filling factor.
- Determination of outer radius according to the necessary inertia and kinetic energy.
- Determination of efficiency and mass for the optimization.

In the design process, it is assumed that iron permeability is infinite ($\mu_r = \infty$) and PM permeability is unit ($\mu_m = 1$).

Magnetic flux density functions in the air gap are achieved by solving Poisson's equation in the polar coordinate system, which is given for SPM machines in [12]. The final equation is given by (1).

$$B_{air}(r,\theta) = \sum_{n=1}^{\infty} 2B_r\alpha_p \frac{\sin(\frac{n\pi\alpha_p}{2})}{(\frac{n\pi\alpha_p}{2})} \frac{np}{np^2-1} R_5^{(1-np)} \times \left\{ \frac{(np-1)R_5^{2np} + 2R_6^{(1+np)}R_5^{(np-1)} - (np+1)R_6^{2np}}{2\left[R_4^{2np} - R_6^{2np}\right]} \right\} \times \left[r^{(np-1)} + R_4^{2np} r^{-(np+1)}\right]\cos(np\theta) \quad (1)$$

where R_2 to R_5 are the radiuses of different parts of machine and being shown in Figure 1. p is the number of pole-pairs. α_p and B_r are PM arc to pole pitch ratio and magnet remanent, respectively. Equation (1) is too complex for a simple design, being deeply dependent upon PM and air gap thickness and it could not be converted into simpler equations. The design and optimization process using such equation will be too complex and time consuming.

On the other hand, in a simple magnetic circuit including an air gap, a unit permeability permanent magnet and an infinite permeability iron core, the flux density in air gap can be calculated as follows [20]:

$$B_p = B_r \frac{L_m}{L_m + L_g} = B_r \frac{R_5 - R_4}{R_5 - R_2} \quad \text{(2-a)}$$

where L_m and L_g are permanent magnet and air gap thickness, respectively. This equation can be rewritten for a *p* pole-pairs machine as (2).

$$B_p = B_r \frac{R_5 - R_4}{R_5 - R_2} \cos(p\theta) \quad (2)$$

Using equation (1), the maximum magnetic flux density in a four pole machine with $R_2=12mm$, $R_4=20mm$, $R_5=24mm$, $r=(R_4+R_2)/2=16mm$, $B_r=1$, $p=2$ and $\alpha_p=0.066$, is 0.35. However, the maximum magnetic flux density calculated using equation (2) is 0.333, which shows 4.6% error for air gap flux density. FEM simulations will show that the errors of the final design are lower than 5% for this machine and this amount of error is acceptable for a simplified design. So, equation (2) is used for the calculation of air gap flux in the analytic design of machine.

The effective air gap in slotless permanent magnet machines is actual air gap plus PM thickness, which is too large in this type of machines. Therefore, the magnetic flux produced by windings is much lower than the flux produced by permanent magnets. Then, the magnetic flux produced by windings can be ignored by a good approximation.

In a *p* pole-pairs machine, the pole area in front of stator can be calculated using (3).

$$A_p = \frac{\pi}{p} R_2 L_r \alpha_p \quad (3)$$

where L_r is the axial length of rotor.

Half of the magnetic flux produced by PMs is passed through each branch of stator and rotor yoke. Then, to keep working flux density below the saturation level of stator, the width of stator yoke is calculated by (4) that can be rewritten as (5).

$$\varphi_s = \frac{\varphi_p}{2} \Rightarrow (R_2 - R_1) L_r B_{\max} = \frac{1}{2}\frac{\pi}{p} R_2 L_r \alpha_p B_p \quad (4)$$

$$\pi R_2 \alpha_p B_p + 2p(R_1 - R_2) B_{\max} = 0 \quad (5)$$

where φ_s is the flux passing through each stator yoke leg and φ_p is the created flux by each rotor pole. B_{max} is the maximum flux density allowed in the stator core and B_p is the flux density of operation point and it is obtained using (2). The term $(R_2\text{-}R_1)$ refers to the stator yoke thickness.

In the same manner, the thickness of rotor yoke can be calculated using equation (6).

$$\pi R_5 \alpha_p B_p + 2p(R_5 - R_6) B_{\max r} = 0 \quad (6)$$

where B_{maxr} is the maximum flux density allowed in rotor yoke and must be kept below the saturation level.

Since equation (2) is independent from the radius, the overall torque and phase-induced voltage can be determined by using $F=liB$ and $E=-lVB$ laws as follows:

$$T = \frac{3}{2}\Psi i_p \quad (7)$$

$$E = \Psi \omega \quad (8)$$

where Ψ depends on machine parameters and is calculated using (8).

$$\Psi = 2pNB_p L_r \left(\frac{R_2 + R_3}{2}\right) \quad (9)$$

N, ω and i_p are coil turn number, angular velocity of rotor and peak current of winding, respectively. Coil current and turn number can be found according to the machine torque and the induced voltage (eq. 7 and 8) for each machine. So, the necessary copper area in a three-phase machine is calculated by (10).

$$A_{cu} = \frac{12pNi_p k_{cu}}{\sqrt{2}ff} \quad (10)$$

Where ff, k_{cu} are filling factor and necessary cupper area for one ampere of current (rms), respectively.

On the other hand according to Figure 1, available copper area is calculated by (11).

$$A_s = \pi\left(R_3^2 - R_2^2\right) \quad (11)$$

By equalizing the necessary and available copper area (10 and 11), equation 12 can be obtained.

$$A_s = A_{cu} \Rightarrow R_3^2 - R_2^2 - \frac{12pNi_p k_{cu}}{\pi\sqrt{2}ff} = 0 \quad (12)$$

By substituting *N* and i_p from (7) and (8) in (12) and by solving (2), (6), (7) and (12) all together, machine dimensions will be found except for the outer radius of flywheel.

The kinetic energy stored on a hollow cylinder can be calculated by using (13) [4].

$$E_n = Pt = \frac{1}{2} I_{total} (\omega_2^2 - \omega_1^2) \quad (13)$$

$$I_{total} = I_{PM} + I_{Fe} + I_{Com} = \frac{1}{2} L_r \pi [D_{PM}\left(R_5^2 - R_4^2\right)^2 + D_{Fe}\left(R_6^2 - R_5^2\right)^2 + D_{Com}\left(R_7^2 - R_6^2\right)^2] \quad (14)$$

Where *En* is the energy stored in EMB, *P* is output power, *t* is operation time (charge or discharge) of EMB, ω_1, ω_2, are rotor lower and higher angular speed and D_{PM}, D_{Fe}, D_{Com} are weight density of PMs, rotor back Iron and flywheel composite, respectively. Finally, solving (14) all machines dimensions is determined. At this point, losses and efficiency can be found according to machine dimensions. In order to calculate losses, first length of each phase winding must be determined by (15).

$$L_{phase} = 4pN\left[(L_r + 2e) + \frac{\pi(R_3 + R_2)}{2p}\right] \quad (15)$$

where *e* is axial length of the end-windings. The resistance of each phase and total copper loss can be calculated by (16), (17).

$$R_{phase} = L_{phase}\rho_{cu} = 4pN\left[(L_r + 2e) + \frac{\pi(R_3 + R_2)}{2p}\right]\rho_{cu} \quad (16)$$

$$P_{cu} = 3R_{phase} i^2 \quad (17)$$

where ρ_{cu} is wire specific resistance.

Iron losses can be achieved from factory datasheets. It is usually given in watt per weight. So, stator mass must be identified for determination of iron losses. It should be noticed that rotor back iron flux is negligible and its losses can be ignored. Stator mass can be calculated by (18).

$$m_{Fe} = Vol_{Fe} D_{Fe} = \pi (R_2^2 - R_1^2) L_r \rho_{Fe} \quad (18)$$

where D_{Fe} is iron weight density. The iron losses can be written as (19) [21].

$$P_{Fe} = m_{Fe} K B_{\max}^{a} F^{b} \quad (19)$$

where *K, a* and *b* can be defined from core material datasheet. Micro-satellite EMBs work in vacuum. So, wind losses are equal to zero. On the other hand, rotor or flywheel is floated by magnetic bearings and the mechanical losses are also zero. Then the efficiency can be written as (20).

$$Eff = \frac{P_o}{P_o + P_{cu} + P_{Fe}} \quad (20)$$

IV. OPTIMIZATION

In design section, the machine dimensions (R_1 to R_7 and L_r) are unknown. R_1 deals with heat pipes and inter-connections. So, R_1 and L_g are defined on the basis of mechanical constraints. On the other hand, the turn number of each coil (N) has to be calculated from given parameters. B_{max} is the final unknown parameter that affects the iron losses of machine. If B_{max} is assumed to be small, machine mass increased and if it is chosen close to saturation level, the iron losses will be increased. Finally we have nine unknown parameters and six equations in the design process (5) to (8), (12) and (14). So, three of the unknown parameters are remaining free and have to be chosen arbitrary. In order to obtain maximum efficiency and minimum mass, three unknown parameters must be optimized. Particle Swarm Optimization (PSO) is the optimization algorithm that is used in this paper. PSO has the advantage of algorithm simplicity, fast convergence, low probability of local convergence and continuity [20]. Efficiency is the objective function and L_r, L_m and B_{max} are optimization variables. Boundaries of the variables are chosen as below:

$$2mm \le L_r \le 100mm$$

$$0.5mm \le L_m \le 10mm$$

$$0.7T \le B_{\max} \le 1.5T$$

Efficiency is proportional to volume and mass in small machines; therefore, the machine mass is selected as the optimization constraint and the maximum acceptable mass for stator is taken 100gr.

Results of optimization and design are given in Table II. In order to show that the unknown parameters are globally optimized, the curve of efficiency with respect to the number of iterations is shown in Figure 3, for ten different start points. As it can be inferred from this figure, it is obvious that all optimizations reach the same point. It should be noticed that the optimized efficiency excludes magnetic bearing and other additional losses.

It should be considered that iron losses are related to the frequency. So, the variables are optimized at the speed of 40000 rpm for overall efficiency optimization.

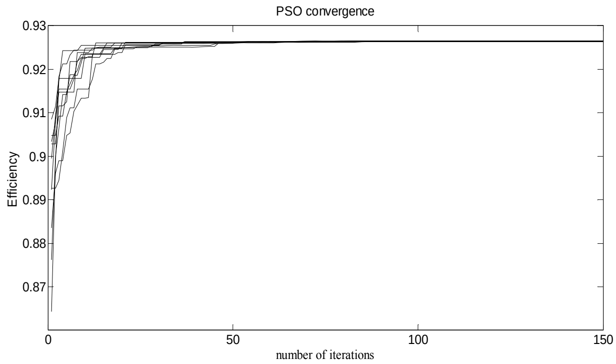

Figure 3. Optimization results for ten run.

TABLE II. OPTIMIZATION AND DESIGN RESULTS FOR SPM MACHINE

Optimization Results				R_2 (mm)	R_3 (mm)
$B_{(max)}$ (T)	L_r (mm)	L_m (mm)	Eff. (%)		
0.9	10.4	4.2	98.2	12.6	25.2
R_4 (mm)	R_5 (mm)	R_6 (mm)	N (Coil turn number)	Mass (Kg)	
26.2	30.4	33.7	36.2	0.175	

V. DESIGN AND VALIDATION BY FEM SIMULATION

Two-dimensional finite element simulations with ANSOFT Maxwell-2D software were carried out for analytical design validation. Two types of simulation are performed for this aim. The first one is the magneto-static simulation which investigates the maximum flux density in the static condition and the second one is the AC simulation that investigates the dynamic performances of machines, like back EMF, dissipations and torque in the nominal speed and frequency. Figure 4 shows the magnetic flux density distribution resulted by magneto-static simulation of machine with parameters given in Tables I and II. It is clear that the flux density in stator of machine is less than 0.9 Tesla, achieved in the optimization process. Figure 5 shows back EMF and produced torque for the machine resulted from AC simulations.

Referring to table I, maximum back EMF of each phase in 40000rpm is 28.7v and the nominal torque is 9.55 (10^{-3}N.m) in this speed. In Figure 5, maximum back EMF of each phase resulted by simulation is 27.6v, and the nominal torque is 8.96 (10^{-3}N.m) that shows 6% and 3.8% errors for produced back EMF and Torque respectively.

VI. CONCLUSION

In this paper, slotless external rotor synchronous permanent magnet machine is designed and optimized. An approximation is used for air gap flux density calculation of the machines for parametric design simplification. The error of this approximation, which simplifies the design process extremely, is less than 6%. Particle swarm optimization was used for optimizing the machine. Static and dynamic finite element simulations were used to validate the design and optimization processes. Simulations confirmed the design accuracy.

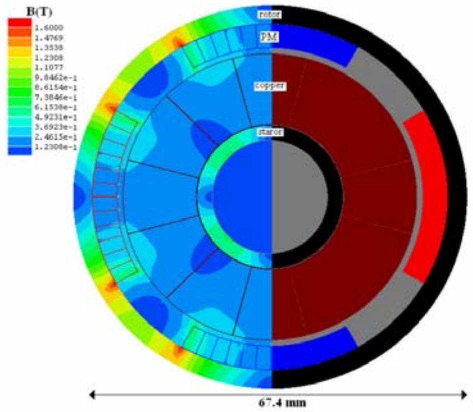

Figure 4. Magnetic flux density distribution resulted by magneto-static simulation.

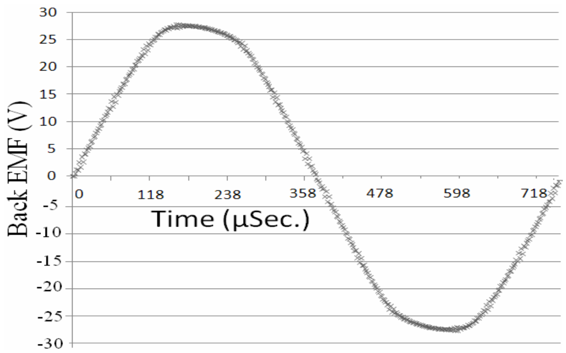

(a)

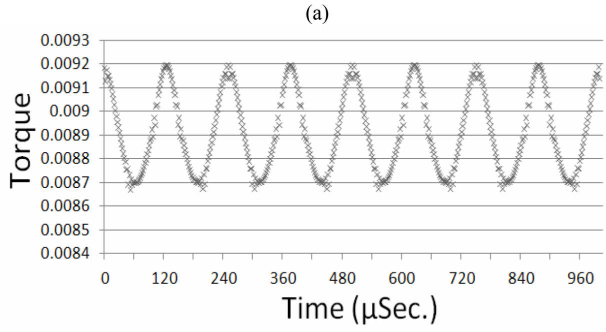

(b)

Figure 5. AC simulation results for the machine
a: Generated Back EMF b: Created torque.

REFERENCES

[1] A. Kirk, P.A. Studer, "Flywheel Energy Storage", Int. J. mech. Sci., VoL 19, pp. 233-245. Pergamon Press 1977.

[2] G.E. Rodriguez, P.A. Studer, D.A. Baer, "Assessment of Flywheel Energy Storage for Spacecraft Power Systems", NASA Technical Memorandum, May 1983.

[3] E. Lee, "A micro HTS renewable energy/attitude control system for micro/nano satellites", IEEE Transaction on Applied Superconductivity, VOL. 13, NO. 2, JUNE 2003.

[4] M. A. Arslan, "Flywheel geometry design for improved energy storage using finite element analysis", ELSEVIER Transaction on material and design, 2007.

[5] W. Wang, "Design of High Speed Flywheel Motor/Generator for Aerospace Applications", Ph.D. dissertation, The Pennsylvania State University, 2003.

[6] B. H. Kenny, P. E. Kascak, R. Jansen, T. Dever, W. Santiago, "Control of a high-speed flywheel system for energy storage in space applications", IEEE Transaction on Industry Applications, VOL. 41, NO. 4, JULY/AUGUST 2005.

[7] A.A. Arkadan, R. Vyas, J.G. Vaidya, M.J.Shah, "Effect of toothless stator design and core and stator conductorseddy current losses in permanent magnet generators", IEEE Transaction on Energy Conversion, Volume 7, Issue 1, Mar 1992.

[8] A. Kaddouri, H. Le-Huy, "Analysis and design of a slotless NdFeB permanent-magnet synchronous motor for direct drive", Industry Applications Society Annual Meeting, Conference Record of the IEEE 1992.

[9] T. Kosaka, N. Matsui, T. Shikayama, R. Oguro, "Drive characteristics of slotless PM motors", IEEE Industry Applications Conference, 1999.

[10] Y. S. Chen, Z. Q. Zhu, D. Howe, "Slotless brushless permanent magnet machines, influence of design parameters", IEEE Transaction on Energy Convertion, Vol. 14. No. 3, September 1999.

[11] N. Bianchi, S. Bolognani, F. Luise, "High Speed Drive Using a Slotless PM Motor", IEEE Transaction on Power Electronics, VOL. 21, NO. 4, JULY 2006.

[12] Zhu, Z.Q. Howe, "D. Instantaneous magnetic field distribution in permanent magnetbrushless DC motors", IEEE Transactions on Magnetics Volume 29, Issue 1, Jan 1993.

[13] S. R. Holm, H. Polinder, J. A. Ferreira, "Analytical Modeling of a Permanent-Magnet Synchronous Machine in a Flywheel", IEEE Transaction on Magnetics, VOL. 43, NO. 5, MAY 2007.

[14] M. Markovic, Y. Perriard, "Simplified Design Methodology for a Slotless Brushless DC Motor", IEEE Transaction on Magnetics, VOL. 42, NO. 12, DECEMBER 2006.

[15] Y.D. Valle ,G. K. Venayagamoorthy,S. Mohagheghi, J. C. Hernandez, R. G. Harley, "Particle Swarm Optimization: Basic Concepts, Variants and Applications in Power Systems", IEEE TRANSACTIONS ON EVOLUTIONARY COMPUTATION, APRIL 2008.

[16] W. Wang, D. Zhong, H. Hofmann, J. Noland, C. E. Bakis "Design of High-Speed Permanent Magnet Machine for Small Flywheel ", 1st International Energy Conversion Engineering Conference, August 2003.

[17] A.S. Nagorny, N.V. Dravid, R.H Jansen, B.H. Kenny, "Design Aspect of a High Speed Permanent Magnet Synchronous Motor/Generator for Flywheel Applications", IEEE International Conference on Electric Machines and Drives, 2005.

[18] M. Popescu, D.M. Ionel, T.J.E. Miller, S.J. Dellinger, M.I. McGilp, "Improved finite element computations of torque in brushless permanent magnet motors", IEE Proc.-Electr. Power Appl., Vol. 152, No. 2, March 2005.

[19] D. M. Ionel, M. Popescu, M. I. McGilp, T. J. E. Miller, S. J. Dellinger, "Assessment of Torque Components in Brushless Permanent-Magnet Machines Through Numerical Analysis of the Electromagnetic Field", IEEE Transaction on Industry Applications, VOL. 41, NO. 5, SEPTEMBER/OCTOBER 2005.

[20] J. F. Gieras, M. Wing, "Permanent Magnet Motor Technology", Design and Applications, Second edition, Marcel Dekker, 2002.

[21] W. G. Hurley, W. H. Wolfle, J. G. Breslin, "Optimized Transformer Design: Inclusive of High-Frequency Effects", IEEE Transactions on Power Electronics, VOL. 13, NO. 4, JULY 1998.